Radio Propagation Model for Long-Range Wireless Sensor Networks

Simon Willis and Cornelis Jan Kikkert
Electrical & Computer Engineering
James Cook University
Townsville, Australia
simon.willis@jcu.edu.au, keith.kikkert@jcu.edu.au

***Abstract*—Wireless Sensor Networks are ideal for monitoring environmental conditions, but typical nodes are limited by their short transmission range. This paper presents a long-range node with a tested range of 13.2 km. A novel radio propagation model is presented, which has been experimentally verified. This paper also presents a unique method to determining the number of multipath signals due to reflection and refraction in a suburban environment.**

***Keywords*—wireless sensor network, radio propagation model, long range**

I. INTRODUCTION

Wireless Sensor Networks (WSN) have emerged as a useful technology for a plethora of sensing applications. Manufacturers such as Crossbow [1] have produced many nodes such as the Mica2 Mote, which are being used by researchers worldwide. A major limitation of existing nodes such as the Mica2 is their maximum transmission range of several hundred meters. This restricts the node to applications that require the monitoring of small geographical areas only.

In countries such as Australia, there is a need to monitor environmental resources over very large areas. Typical examples are the monitoring of the water-level in a cattle feeding trough and the monitoring of the temperature and salinity of water on the Great Barrier Reef. To overcome the limitation in transmission range we have developed a wireless sensor node called the JCUMote, which operates in a licence free 40 MHz band, which in Australia permits a 1 W effective radiated power.

When operating a WSN over a large area it is important to use a good radio propagation model to determine the performance of the links. The model must include the effects of irregular terrain and multipath reflections. To perform this task we have developed a radio propagation model specifically for use with wireless sensor networks, called the JCU-WSN Model.

To verify the performance of the JCU-WSN model we have conducted field tests of the JCUMotes in rural and suburban areas and have compared the results with JCU-WSN model predictions. Using these results we have created an additional model that will estimate the number of multipath reflections in an urban environment.

II. RADIO PROPAGATION MODEL

Radio propagation has been the subject of research for a long period of time. The focus of more recent work has been on predicting the signal strength in an urban environment for digital television and mobile phones. Our scenario is very different, since the sensor nodes operate at a lower frequency and will often be deployed in a sparsely vegetated, rural environment. This section describes the typical propagation mechanisms that are likely to occur at the proposed frequency with elevated nodes.

A. Radio Propagation Modelling

1) Radio Propagation Over Flat Terrain

When a radio signal is transmitted over flat terrain it is subject to attenuation due to free-space loss, ground reflections and refraction due to the Earth's surface. The free-space model calculates the decrease in signal strength due to the distance away from the transmitter and shows that the received signal strength is proportional to the inverse square of the distance.

When an antenna is elevated, a ground reflection also occurs. The magnitude of the reflected power depends on the angle of incidence and the ground conductivity. At the receiver, the ground reflection is out of phase with the line-of-sight signal and causes cancellation. Hernando and Pérez-Fontán [2] shows that this can be approximated by the Plane-Earth model (equation 1), where the received signal is inversely proportional to distance raised to the fourth power.

$$P_r = P_t G_t G_r \left(\frac{h_t h_r}{d^2} \right)^2 \quad (1)$$

Due to a variation in the atmosphere's refractive index with height, the radio signal follows a curved path and tends to follow the curvature of the Earth. This effectively lengthens the range of a transmitter beyond the horizon. In propagation studies [2], straight lines are used for the propagation paths and the Earth is assumed to have an effective radius given by kR_0, where R_0 is the radius of the earth (6370km) and k is a correction factor, which is normally 4/3.

2) Radio Propagation Over Irregular Terrain

Irregular Terrain inside the Fresnel zone of the direct path causes attenuation of the signal due to scattering. Several models exist, which attempt to calculate these losses. The JCU-WSN model uses the point-to-point (PTP) model, developed by Wong [3]. The path loss due to scattering depends on refractive effects and is thus different from node A to node B and from node B to node A.

3) Multipath Reflections

Reflections can be caused by obstacles which are bigger than the signal wavelength. These reflections will arrive at the receiver with different phase and magnitude to the line-of-sight ray and can cause cancellation of the signal.

B. The JCU-WSN Model

The JCU-WSN model accounts for the above propagation characteristics as described by the authors in [4]. The model calculates the effects of the terrain, by using a terrain profile along the line of sight path, which can be obtained from digital elevation data provided by NASA [5]. The model assumes the terrain is symmetrical along the x-axis as shown in Fig. 1.

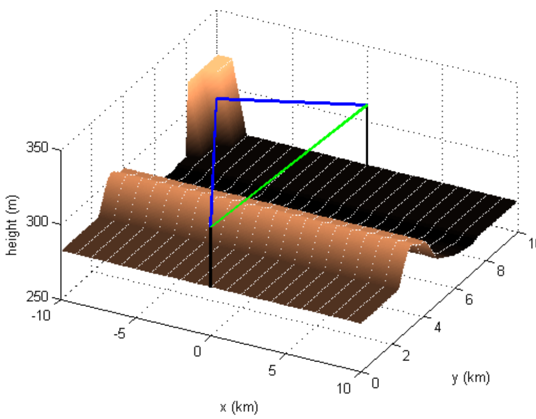

Figure 1. Terrain used for multipath signals, the terrain along x=0 is the actual path profile.

To represent multipath reflections, the model randomly places reflectors on the terrain, as shown in Fig. 1, and calculates the received signal strength. If the magnitude of the reflection is more than 30 dB below the direct signal, then it is discarded and recalculated for a new position. The number of multipath reflections is specified by the user and is effected by large terrain obstacles and buildings.

III. The Long-Range Wireless Sensor Node

A long-range wireless sensor node, called the JCUMote, was designed and is discussed by the authors in [6]. The JCUMote operates at a frequency of 40.66-41 MHz with 1 W EIRP. The node is based on the Crossbow Mica2 Mote [1], which is used extensively by other researchers. The Mica2 has an open-source schematic and can be programmed using TinyOS [7], which has been developed specifically for WSNs. By basing the JCUMote on this node we were able to re-use existing protocols and applications available in TinyOS.

The block diagram of the JCUMote is shown in Fig. 2. This node uses the same ATMEL ATmega128L microprocessor as the Mica2. The node contains 4Mb flash memory and an expansion port for connecting programming or sensor boards.

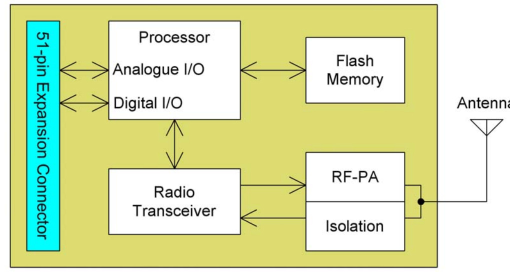

Figure 2. The JCUMote Block Diagram

For operation at 40 MHz, the JCUMote uses a different radio transceiver than the Mica2. A Melexis TH7122 was chosen as it contains an FSK modulator and demodulator. This IC is capable of operation between 27 MHz and 1 GHz and was configured for operation at 40 MHz using external circuitry. The TH7122 is capable of producing +10 dBm (10 mW) of RF power, which is amplified to +30 dBm (1W) using a custom-designed class-C power amplifier (PA) built from discrete components. The PA was designed using Microwave Office and is stable over a broad frequency range.

The JCUMote uses a single antenna to both transmit and receive. When transmitting, the 1 W power output is potentially damaging to the receiver front-end. Therefore, an isolation network was developed, which prevents the transmitted signal reaching the receiver circuitry.

The modulation hardware was configured for a frequency deviation of 38.4 kHz, so that the 9600 bps Manchester encoded data occupies a 150 kHz channel bandwidth. This allows 2 channels in the 40.66 – 41.0 MHz band, if required. The transmitted frequency spectrum is shown in Fig. 3. To protect the spectrum analyser, a 20 dB attenuator was used.

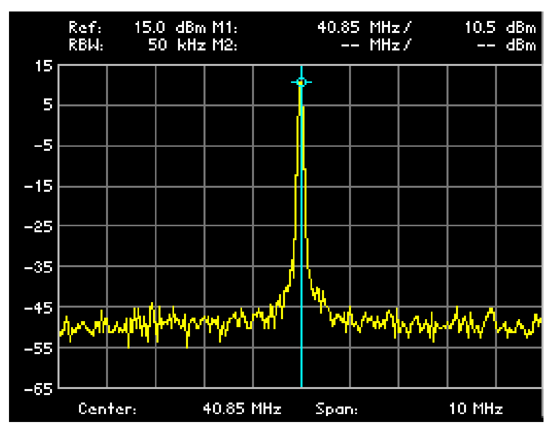

Figure 3. Frequency spectrum (20 dB attenuated)

For modulation, the digital waveform is injected into the control voltage input of the VCO (voltage controlled oscillator) of the Melexis TH7122. This form of modulation does not allow data with a DC component to be transmitted due to the feedback mechanism of the PLL. Hence, Manchester encoding was used. Since the TH7122 only provides a basic bit-level interface for transmitted and received data, the Manchester encoding was performed using algorithms in TinyOS.

The receiver was measured to have a sensitivity of -80 dBm at a 3×10^{-3} bit error rate, 20 kbps data rate and 20 kHz frequency deviation. At 40 MHz the background noise level on the outskirts of a suburban area was measured to be -95.8 dBm over a 100 kHz bandwidth, which is far higher than the sensitivity quoted for the Melexis TH7122, so that the range of the transmitter is primarily determined by man made noise. Fig. 4 shows the JCUMote PCB.

Figure 4. The JCUMote PCB

The design of the antenna was also investigated. The aim of this design was to be low in cost, highly efficient and suitable for WSNs. Nodes in a WSN must communicate with nodes in all directions, hence the antenna must be omni-directional. The final design consists of a quarter-wavelength whip antenna surrounded by 4 quarter-wavelength radials at a 30^o declination to the horizontal (Fig. 5). This antenna has an input impedance of 49 + j3 Ω, with a return loss of -31 dB at 40.84 MHz.

The JCUMote is powered by a 6 V lead-acid battery and has been tested with a solar panel. The node is housed in an aluminium enclosure as shown in Fig. 5. The antenna is mounted to the top of the enclosure with the radials extending from the base.

Figure 5. Node installed with radials

IV. Field Testing

A. Rural Environment

The range of the nodes was determined in a rural setting by measuring the received signal strength at set distances from the transmitter. A transmitting node was programmed using TinyOS to produce a simple known data stream, four times per second. A receiving node was programmed with a TinyOS application which logged the received signal strength, noise level and packet loss to a connected laptop computer.

The transmitter was installed at the top of a mountain range, which was 290 m above the final receiver testing position. The transmitter was mounted on a 1.8 m star-picket, surrounded by four quarter-wavelength radials. Periodic measurements were taken at the locations shown in Fig. 6, using the receiving node mounted on a car roof. The maximum range was measured to be 13.2 km.

Figure 6. Receiver Test Positions (Google Earth)

The JCU-WSN model was used to calculate the mean signal strength (taken over 1000 runs) for cases where there are between 0 and 5 multipath reflections. A comparison between the JCU-WSN model predictions and the measured signal strength are shown in Table I. It is obvious that in all cases the model is most accurate for the case of a direct ray and one ground reflection only. This would be the expected case, because there are no buildings or large terrain features in the test area that may cause reflections.

TABLE I. Measured and Predicted Signal Strength

Posn.	pR_{meas} (dBm)	Dist. (km)	WSN Model (mean dBm) *Num. reflections*			Plane-Earth Model (dBm)
			0	*1*	*2*	
1	-56.3	2.8	-46.2	**-54.6**	-54.5	-55.1
2	-80.3	4.0	-50.6	**-61.0**	-60.9	-60.6
3	-67.3	5.5	-54.3	**-66.8**	-66.6	-65.8
4	-70.4	6.7	-56.5	**-70.4**	-70.2	-69.1
5	-73.8	8	-58.5	**-73.6**	-73.2	-72
6	-77.2	10.1	-60.9	**-77.6**	-77.0	-76
7	-76.3	11.2	-63.5	**-81.0**	-80.4	-77.7
8	-77.5	12.2	-64.7	**-82.8**	-81.8	-79.2
9	-84.2	13.2	-65.6	**-84.2**	-83.1	-80.4

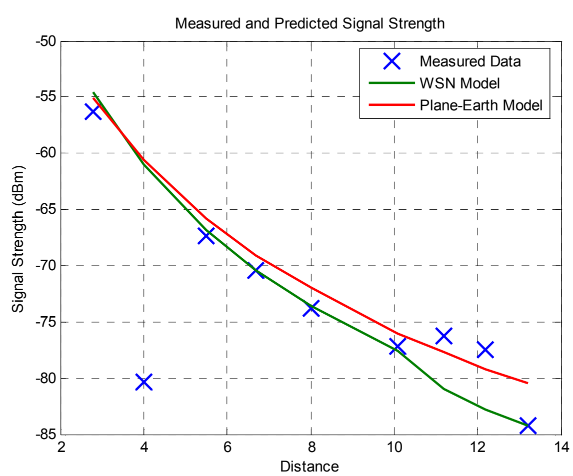

Figure 7. Comparison of Results for Rural Tests

A comparison between the measured results, the JCU-WSN model with 1 ground reflection, and the plane-earth model is shown in Fig. 7. It is evident that the JCU-WSN model gives a more accurate prediction than the plane-earth model. Fig. 7 shows an anomaly at 4 km, which is due to a line of sight obstruction that was not evident in the terrain data.

B. *Suburban WSN Testing*

Four nodes were constructed and installed in a suburban area to test the functionality of the nodes as an ad-hoc network. A TinyOS application was written which allowed each node to log the received signal strength of neighbouring nodes and forward the measurement to a base station node every eight seconds. The base station was connected to a PC running Crossbow's MoteView software [1] which continuously logs readings into a connected database. Measurements were taken over a period of 41 days, over which time 930 000 records were logged in the database.

The base station node was installed on the roof of the Electrical & Computer Engineering building at James Cook University at an elevation of 10 m above ground. Three other sensor nodes were installed in a neighbouring suburb on the roof of houses on top of existing television antennae, approximately 4 m above ground. The complete network is shown in Fig. 8 where node 0 is the base station node. The link between nodes 0 and 4 is 3.1 km long and is shown as a dashed line because that path is obstructed by a small hill, so that the link only operated occasionally.

Figure 8. Suburban Wireless Sensor Network (Google Earth)

The measured signal strength for each link is shown in Table II, where pR_{meas} is the measured signal strength and pR_{mean} is the mean predicted signal strength after 1000 simulations of the JCU-WSN Model. For each link the optimum number of reflections is highlighted in grey. The worst prediction was within 2.5% of the measured value (4→1), all the others were more accurate. It is obvious that in a suburban environment there are a larger number of reflections than in a rural environment. This is to be expected due to the presence of surrounding buildings. The received power measurements show that links are asymmetrical, due to diffraction. For example, the link between nodes 3 and 4 has a difference of 2 dB in each direction. Note: Node 1 emits 4 dB less power than other nodes.

V. Predicting the Number of Multipath Signals

Table II showed that the number of multipath signals due to reflection and diffraction has a strong influence on the accuracy of the model. It is also evident that the number of multipath signals is difficult to determine due to the paths being partially obstructed by houses, causing significant diffraction.

To enable the number of multipath signals to be estimated an empirical model was developed based on the results presented in Table II. The model uses three parameters to determine the number of multipath signals: 1) the number of buildings in the Fresnel zone, 2) the height of the receiving node and 3) the distance of the closest building to the receiver.

Table III shows the number of multipath signals (ground reflection excluded) for each link and the number of buildings in the Fresnel zone (counted using Google Earth). Generally, links with fewer buildings have less multipath signals.

Table III also includes the receiver height. It implies that when a receiver is elevated it receives additional multipath signals. An example is the link between nodes 0 and 4. When the higher node (0) is receiving more multipath components are present than when the lower node (4) is receiving. However the shape of the hill partially obstructing that path and the diffraction that causes may be more dominant.

Table III also shows the distance from the receiver to the closest building in the Fresnel zone. It was noticed that additional multipath signals are received when a building is in close proximity to the receiver. An example of this is the link between nodes 3 and 4. Node 3 is closer to a building (10 m) than node 4 (50 m). When node 3 is receiving, more multipath signals are present than when node 4 is receiving.

TABLE II. Measured and Predicted Signal Strength (Suburban Tests)

Link	pR_{meas} (dBm)	Dist. (km)		WSN Model						Plane-Earth model
			Num. signals	***0***	***1***	***2***	***3***	***4***	***5***	
0→3	-67.3	1.9	pR_{mean} (dBm)	-47.4	-69.5	**-67.8**	-66.1	-64.6	-63.3	-54.7
0→4	-77.0	3.1	pR_{mean} (dBm)	-53.2	-80.4	**-77.1**	-74.0	-71.8	-70.3	-64.4
1→3	-73.5	1.4	pR_{mean} (dBm)	-52.8	-81.8	-75.7	**-72.0**	-69.4	-68.4	-66.1
1→4	-68.6	0.6	pR_{mean} (dBm)	-40.2	**-68.8**	-64.2	-60.9	-59.0	-57.9	-61.0
3→0	-68.2	1.9	pR_{mean} (dBm)	-47.4	-69.6	**-68.0**	-65.9	-64.4	-63.7	-54.7
3→4	-67.7	1.5	pR_{mean} (dBm)	-47.8	-78.0	-71.2	**-67.8**	-65.7	-64.3	-63.7
4→0	-75	3.1	pR_{mean} (dBm)	-54.2	-81.4	-78.4	**-75.0**	-73.6	-71.9	-64.4
4→1	-62.9	0.6	pR_{mean} (dBm)	-40.2	**-64.5**	-59.8	-56.4	-54.4	-53.2	-61.0
4→3	-66.2	1.5	pR_{mean} (dBm)	-48.4	-78.6	-72.3	-67.9	**-65.6**	-64.3	-63.7

TABLE III. SUBURBAN LINKS SHOWING NUMBER OF BUILDINGS AND THE CLOSEST BUILDING

Num. Signals	Link	Dist. (km)	Num. Buildings	Closest Building (m)	Closest Building (%)	Rx Height (m)
0	1→4	0.6	9	40	6.7	3.6
	4→1	0.6	9	80	13	4
1	0→3	1.9	9	40	2.1	4.8
	3→0	1.9	9	120	6.3	13
	0→4	3.1	11	60	1.9	3.6
2	4→0	3.1	11	120	3.9	13
	1→3	1.4	16	10	0.71	4.8
	3→4	1.5	23	50	3.3	3.6
3	4→3	1.5	23	10	0.67	4.8

These observations were used to create an empirical model. The model uses three steps. The first step applies a building correction multiplier to account for the immediate buildings surrounding the receiver. The closeness of a building is expressed as a percentage relative to the path length. If the relative closeness is greater than 5%, then the node is classed as 'open'. Conversely, if the relative closeness is less than 2 % then the node is classed as 'confined'. To compensate, the number of buildings is reduced or increased by 20% for open and confined nodes, respectively.

Following the building compensation, the model calculates the number of multipath signals by applying the corrected number of buildings to equation (2). This equation was developed as the line of best fit for all links of normal height (links with a receiver dramatically above or below the mean building height were ignored). The resulting line of best fit is shown in Fig. 9 and is defined by equation (2).

$$m \approx {}^{b}\!/_{8} - 0.6 \qquad (2)$$

Where m is the number of multipath signals and b is the corrected number of buildings on the path.

The final stage of the model compensates for elevated receivers by adding or subtracting 1 multipath signal for high or low receivers, respectively. A high receiver is classed as having an elevation greater than twice the average height of the surrounding buildings. Low receivers are classed as having a height less than half of the average surrounding buildings.

This model was implemented as a MATLAB function and has been tested to accurately predict the correct number of multipath components for all links in Table II, as well as for some further "car-roof" tests that were performed in the same suburb.

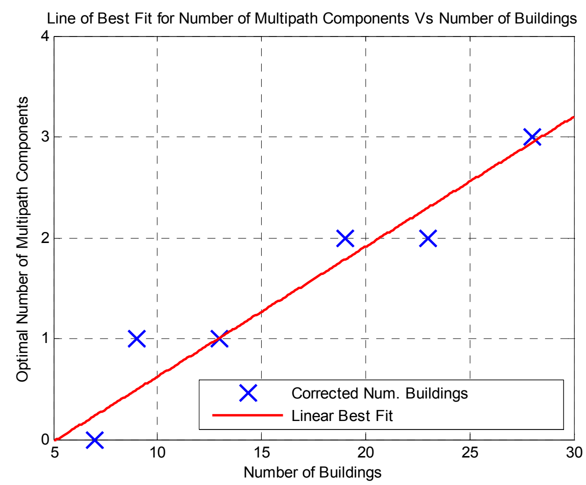

Figure 9. Line of Best Fit for Number of Multipath Signals Vs Number of Buildings

ACKNOWLEDGMENT

The authors wish to thank the staff at James Cook University for their support in manufacturing the hardware. The authors thank AWR for their University support program, which made it possible to use Microwave Office for hardware simulations. The Australian Research Council (ARC) is acknowledged for providing the grant for the equipment used for making the measurements of the hardware.

REFERENCES

[1] (2007, January 23). Crossbow Technology : Wireless Sensor Networks : Home Page [Online]. Available: http://www.xbow.com/Home/HomePage.aspx

[2] J. M. Hernando and F. Perez-Fontan, Introduction to Mobile Communications Engineering. Boston, USA: Artech House, 1999.

[3] H. Wong, (2004, November 04). Field Strength Prediction in Irregular Terrain - the PTP Model [Online]. Available: http://www.fcc.gov/oet/fm/ptp/report.pdf

[4] S. L. Willis and C. J. Kikkert, "Radio Propagation Model for Long-Range Ad Hoc Wireless Sensor Network," presented at 2005 International Conference on Wireless Networks, Communications and Mobile Computing, Maui, Hawaii, 2005.

[5] E. Ramirex, (2007, January 30). Shuttle Radar Topography Mission [Online]. Available: http://www2.jpl.nasa.gov/srtm/

[6] S. L. Willis and C. J. Kikkert, "Design of a Long-Range Wireless Sensor Node," presented at IEEE International Conference on Circuits and Systems, Singapore, 2006.

[7] (2004, June 22). TinyOS [Online]. Available: http://www.tinyos.net/